Forest Ecology and Management 469 (2020) 118159

Contents lists available at ScienceDirect

Forest Ecology and Management

journal homepage: www.elsevier.com/locate/foreco

Differential effects of drought on nonstructural carbohydrate storage in seedlings and mature trees of four species in a subtropical forest

Peipei Zhang[a], Xuhui Zhou[a,b], Yuling Fu[a,*], Junjiong Shao[a], Lingyan Zhou[a], Songsong Li[a], Guiyao Zhou[a], Zhenhong Hu[c], Jiaqi Hu[a], Shahla Hosseini Bai[d], Nate G. McDowell[e]

[a] Tiantong National Forest Ecosystem Observation and Research Station, Center for Global Change and Ecological Forecasting, Shanghai Key Lab for Urban Ecological Processes and Eco-Restoration, School of Ecological and Environmental Sciences, East China Normal University, Shanghai 200062, China
[b] Shanghai Institute of Pollution Control and Ecological Security, 1515 North Zhongshan Rd, Shanghai 200437, China
[c] College of Natural Resources and Environment, South China Agricultural University, Guangzhou 510640, China
[d] Faculty of Science, Health, Education and Engineering, University of the Sunshine Coast, Maroochydore DC, QLD, 4558, Australia
[e] Pacific Northwest National Laboratory, Richland, WA 99352, USA

ARTICLE INFO

Keywords:
NSC
Subtropical evergreen trees
Throughfall exclusion
Tree life stages
Understory seedlings

ABSTRACT

Nonstructural carbohydrates (NSC) play important roles in forest vulnerability to climate change, especially under increasing drought intensity and frequency. Understanding NSC dynamics is essential for accurately predicting the resistance and resilience of forests in response to drought. However, our knowledge of NSC responses to drought is still limited due to the lack of research in trees of different life stages. In this study, we conducted a throughfall exclusion experiment (TFE) with four subtropical evergreen tree species to examine drought effects on NSC in mature trees and understory seedlings. Our results showed the differential effects of drought on NSC dynamics of understory seedlings and mature trees. In the TFE experiment, mature trees of all four species were relatively homoeostatic with the insignificantly changed NSC pools, photosynthesis, and growth under the drought treatment compared to the control. In contrast, understory seedlings displayed significant decreases in total NSC and soluble sugars ($-14.70 \pm 3.66\%$ and $-16.93 \pm 3.85\%$, respectively) with the exception of *Lithocarpus glaber* (*L. glaber*). The seedlings of *L. glaber* with the highest hydraulic resistance maintained or slightly increased NSC and its components in response to drought. Our study highlights the importance of life stage in assessing drought effects of trees on NSC storage and then forest C cycling, which could be incorporated into the dynamic global vegetation models (DGVMs) to better understand drought effects on forest C balance in the future.

1. Introduction

Forest mortality is an emerging issue due to increased intensity and frequency of drought events coupled with warmer temperature (IPCC, 2014; Allen et al., 2015), altering forest structure, function and service (Allen et al., 2010; Anderegg et al., 2013; Kurz et al., 2008; Phillips et al., 2009). These threats reinvigorated interest in understanding physiological mechanisms underlying tree responses to drought (Hartmann et al., 2015; McDowell et al., 2013; McDowell and Sevanto, 2010). Nonstructural carbohydrates (NSCs) are distributed from leaves and stored into different tissues typically in the form of sugars and starch. NSCs play an important role in tree drought resistance and resilience (O'Brien et al., 2014) by acting as a mobilized carbon (C) resource to support multiple functions in basic metabolism, defense and osmotic adjustment (Chapin et al., 1990). NSC storage in trees can buffer the imbalance between photosynthetic supply and metabolic demand on various timescales from minutes to decades, allowing trees to survive under ominous conditions like drought in the future (Furze et al., 2019). Thus, better knowledge of tree NSC dynamics is important to accurately predict trees' performance and survival under drought (Dietze et al., 2014; Hartmann et al., 2018).

NSC responses to drought largely vary depending on the balance of C assimilation, C storage mobilization, and C demands (Hoch, 2015; McDowell et al., 2011a). NSC concentrations were indicated to increase under mild water stress due to the faster decline of growth than photosynthesis, but may decline when suffering extreme drought due to the prolonged suppression of photosynthesis and the utilization of stored C for meeting C demands (e.g., respiration, metabolism, and defense; Hoch, 2015; McDowell et al., 2011a). Hydraulic failure with insufficient NSC availability during drought condition is assumed to cause

* Corresponding author at: School of Ecological and Environmental Sciences, East China Normal University, 500 Dongchuan Road, Shanghai 200241, China.
E-mail address: ylfu@re.ecnu.edu.cn (Y. Fu).

https://doi.org/10.1016/j.foreco.2020.118159
Received 15 November 2019; Received in revised form 6 April 2020; Accepted 14 April 2020
Available online 20 May 2020
0378-1127/

tree death (McDowell et al., 2011a; Sala et al., 2010). However, the role of carbon starvation in drought-induced tree mortality is still debated as C depletion is not ubiquitously observed at tree mortality (Adams et al., 2017). Under drought, the NSC accumulation, specifically soluble sugars, can maintain high osmotic pressure to prevent turgor loss during drought (O'Brien et al., 2014). Evidence from aspen trees in complete darkness showed that large amounts of sugars were not available for remobilization, which is probably associated with the observed high NSC concentrations in trees under extreme drought (Wiley et al., 2019). These processes are often used to explain the inconsistent responses of NSC concentrations to drought, from declines (Dickman et al., 2015; Maguire and Kobe, 2015; Rosas et al., 2013) to no change (Dickman et al., 2019; McDowell et al., 2019; Rowland et al., 2015) and increases (Galvez et al., 2011; Gruber et al., 2012; Piper et al., 2017). Furthermore, the discrepancies in NSC behaviors in response to drought can be attributed to species-specific variations such as rooting depth, drought resistance ability, and phenological development as well as artificial results of unnatural experimental conditions (Adams et al., 2017, 2015; Mitchell et al., 2014; Nardini et al., 2016; O'Brien et al., 2015; Piper, 2011). The drought-induced reduction in NSC was more common for gymnosperms than angiosperms under tree mortality, since gymnosperm trees with higher xylem embolism resistance had relatively greater NSC (Adams et al., 2017).

Differences in tree life stages have long been ignored when we extrapolated drought responses of NSC in individual trees to forest stand, despite the fact that large trees have been observed with higher mortality rates under drought (Bennett et al., 2015; McDowell et al., 2018). This problem arises because field experiments are dominated by those conducted on seedlings, while experimental manipulation of mature trees is challenging and only rarely attempted (Adams et al., 2017; Hartmann et al., 2018). On one hand, the allometric proportions, photosynthetic capacities, phenological development, and growth rates differ between seedlings and mature trees (Augspurger and Bartlett, 2003; He et al., 2005; King, 2011; Mencuccini et al., 2005; Thomas and Winner, 2002), resulting in variation in C storage and allocation (Hartmann et al., 2018). Previous studies found that seedlings have higher NSC concentrations but with smaller and more fluctuating NSC pools compared to mature trees, which might lead to faster depletion of NSC in seedlings (Baber et al., 2014; Hartmann et al., 2018; Niinemets, 2010). Mature trees are more hydraulically vulnerable with wider conduits (Olson et al., 2018), and undergo stronger inherent hydraulic stress because of larger evaporative demand and longer-distances to transport water (McDowell et al., 2011b; Zhang et al., 2009). On the other hand, understory seedlings experience lower light irradiation and higher humidity than mature trees, but have lower stem water reserves (Oberhuber et al., 2015). Their root networks are limited and almost all roots occur in shallower soil layers, which may make them suffer more serious water shortage than mature trees (Cavender-Bares and Bazzaz, 2000; Mueller et al., 2005; Zweifel et al., 2000). These changes in intrinsic C storage processes, microclimate, and environmental stresses across tree life stages cause uncertainty when extrapolating NSC responses from seedlings to mature trees. Therefore, to link the differential NSC responses with tree sizes, it is necessary to conduct manipulative experiments or long-term observations to examine drought effects across tree life stages (Hartmann et al., 2018).

To date, no study has yet examined drought effects on NSC in mature trees and seedlings in the field at the same time. Here, we carried out a field throughfall exclusion experiment (TFE) in a natural subtropical evergreen forest to explore the drought impacts on whole-tree NSC dynamics as well as the differences of NSC responses in two tree life stages for four species. Specifically, this study aimed to compare NSC responses to drought for co-occurring mature trees and understory seedlings, and examine species variations in NSC responses to drought. We hypothesized that (i) foliage NSC of seedlings will decline more than those of mature trees in response to reduced soil water, and (ii) NSC responses to drought are species-specific in four coexisting subtropical evergreen broadleaf tree species. We stress that our goal is not to detect the ontogeny effect on NSC responses to drought, but to compare the actual responses of mature trees and seedlings growing in the same stand under the simulated drought treatment, offering the potential for improving understanding of forest succession and regeneration in the future.

2. Materials and methods

2.1. Study site

A field study was conducted in Tiantong National Forest Park (29°48′N, 121°47′E, 200 m a.s.l) located in Zhejiang province, Eastern China. The area has a typical subtropical monsoon climate with hot, humid summers and cool, dry winters. Average annual temperature is 16.7 ± 0.8 °C (standard deviation) ranging from 4.9 ± 1.4 °C in January to 28.4 ± 1.3 °C in July, and mean annual precipitation is 1376.0 ± 224.7 mm, which mainly occurs from June to August (1962–2012, data from Tiantong weather station). The mean annual relative humidity is 78 ± 3.7% (Zhou et al., 2017). The soil pH ranges from 4.4 to 5.1 (Yan et al., 2006). The zonal vegetation type is subtropical evergreen broadleaved forests. The dominant tree species in the canopy and sub-canopy include *Schima superba* Gardner and Champ. *Lithocarpus glaber* (Thunb.) Nakai., *Castanopsis sclerophylla* (Lindl.) Schott. and *Symplocos setchuensis* Brand.

2.2. Experimental design and sampling

The throughfall exclusion experiment (TFE) was established in July 2013, containing three blocks with three plots in each block (an area of 25 m × 25 m for each plot). Plots within each block are randomly assigned to one of three treatments, thus each treatment has three replicates. The treatments are (i) TFE plots with transparent concave polycarbonate (PC) plates and gutters placed at a height of 2 m from the ground to exclude approximately 70% of the precipitation, (ii) TFE-control plots that were similar to the drought plots except for the concave side of gutters facing down, hence they did not exclude rain, (iii) ambient plots that were left in their natural state (shown in Fig. S1). Photosynthetically active radiation (PAR) of plots under transparent PC plates was not significantly different from that of the control. Stand canopy openness is 12.4%, and total amount of sun radiation and PAR in understory on sunny days is 78.4%, 81.6% lower than that in the canopy layer, respectively (Xu, 2008).

Mature trees (70–80 years old) and understory seedlings (< 2 m in height, 3–6 years old) of four dominant species *S. superba, L. glaber*, *C. sclerophylla* and *Castanopsis carlesii* (Hemsl.) Hayata were chosen at each plot with two replicated individuals for a total sample size of six individuals per size class, species, treatment and sampling time. These four coexisting evergreen broadleaf tree species in the subtropics were characterized by different hydraulic traits, among which the *L. glaber* trees had the highest dehydration tolerance and the maximum xylem conductance (Kröber et al., 2015; Zhang et al., 2012; Table S1). Seedlings of the four species were shade-tolerant, and most of their fine roots were observed to distribute at the soil depth of 0–20 cm (Zeng et al., 2008). Stem diameters ranged from 12.6 cm to 43.9 cm in the sampled mature trees at breast height, and from 0.8 cm to 2.6 cm in the sampled seedlings at 15 cm height (Table 1). Field sampling was implemented four times over 2015 and 2016. Mature trees of *S. superba* and *L. glaber* were sampled in quarterly intervals from June (June, August, October in 2015 and January in 2016). All remaining individuals (trees and seedlings) for all species were collected in quarterly intervals from August (August, October in 2015 and January in 2016). For mature trees, a stemwood core to the pith was taken with an increment borer (4.3 mm in diameter) at about 1.3 m above the ground on the south face of the tree. In our prior study by staining method on tree cores, the sapwood depths in the target *S. superba*, *L. glaber* and *C.*

Table 1
Basic characteristics of the sampled trees in four species in this study.

Tree life stage	Species	Stem diameter (cm)			Tree height (m)		
		TFE	TFE-control	Ambient	TFE	TFE-control	Ambient
Mature trees	*Schima superba*	20.4 ± 1.9	16.4 ± 1.4	16.9 ± 1.6	12.3 ± 1.1	11.7 ± 1.3	10.1 ± 1.1
	Lithocarpus glaber	15.7 ± 1.1	15.9 ± 0.9	16.2 ± 1.2	12.4 ± 1.4	12.5 ± 0.4	10.8 ± 0.8
	Castanopsis carlesii	36.2 ± 3.3	31.5 ± 2.0	36.7 ± 2.3	15.4 ± 0.4	14.7 ± 1.0	14.2 ± 1.6
	Castanopsis sclerophylla	19.0 ± 0.4	18.5 ± 3.0	20.1 ± 3.4	11.0 ± 0.5	10.3 ± 1.7	11.6 ± 1.6
Seedlings	*Schima superba*	1.6 ± 0.1	1.4 ± 0.1	1.7 ± 0.2	0.7 ± 0.1	0.6 ± 0.1	0.6 ± 0.1
	Lithocarpus glaber	1.0 ± 0.1	1.1 ± 0.1	1.3 ± 0.1	0.7 ± 0.1	0.8 ± 0.1	0.7 ± 0.1
	Castanopsis carlesii	1.6 ± 0.2	1.6 ± 0.1	1.7 ± 0.2	0.7 ± 0.1	0.8 ± 0.1	0.8 ± 0.1
	Castanopsis sclerophylla	2.1 ± 0.3	2.0 ± 0.3	1.9 ± 0.2	0.8 ± 0.1	0.9 ± 0.1	0.7 ± 0.1

Mean values ± SEs (n = 6) are shown. Stem diameter was measured at breast height (1.3 m) and 15 cm height for mature trees and seedlings, respectively.

sclerophylla trees were estimated ranging from 3.05 cm to 4.83 cm, while the sapwood depths in the target *C. carlesii* trees ranged from 6.20 cm to 8.15 cm. Outer dead bark was removed and wood cores (cork cambium to pith) were cut into three sub-cores by distance from the outer wood: 0–3 cm, 3–6 cm and 6 cm-pith stemwood. Through excavation, coarse roots with the diameter around 1 cm were sampled by following the main roots to the distance of 40 cm from the stem base. Fine roots (< 2 mm in diameter) of the sampled individual trees were collected around the sampled coarse roots. Fully sunlit branchlets together with leaves were sampled from mature trees using a pole pruner. To avoid destructive damage on seedlings, only current-yr-old twigs with leaves were sampled from seedling individuals using a pruning shear. Branches with leaves as well as root and stemwood samples were immediately placed in a cooler (0–4 °C) once collected. For each time sampling, branchlet samples were collected during 12:30–14:00, stem/root samples were collected on the same day, and they were taken back to the laboratory within 3 h after sampling.

2.3. Measurement protocols

2.3.1. Microclimate and soil moisture

The microclimate, including air temperature, relative air humidity (RH%), and daily precipitation near plots were recorded automatically by the micrometeorological station (CR1000, Campbell Scientific Inc., Logan, UT, USA) throughout the study period. Sensors were installed at the height of 3 m within canopy. Continuous data were summed (precipitation) or averaged over 30 min intervals. Vapor pressure deficit (VPD) was calculated from records of air temperature and RH% using the equation given in Hartmann (2016), with 30-minute data averaged up to daily means. Volumetric soil water content (VWC%) was recorded in each plot at depths of 5 cm, 15 cm, 30 cm, 50 cm and 75 cm (n = 3 sensors per soil depth for each plot). VWC% under each treatment was calculated by averaging the daily means of measurements from the three replicate plots.

2.3.2. Gas exchange

To enable further interpretation of the carbon balance in trees, we measured gas exchange of the plants during the sampling campaigns. Light-saturated photosynthesis (A_{sat}) was measured with a portable photosynthesis system equipped with a red-blue LED source (LI-6400XT, LI-COR Inc., Lincoln, NE, USA). Reference [CO_2] was matched to ambient conditions and the flow rate was kept at 500 μmol s^{-1}. The cuvette temperature was maintained at 20 °C. A_{sat} of understory seedlings was measured *in situ* with a photosynthetic photo flux density (PFD) of 800 μmol m^{-2} s^{-1}, while that of mature trees was measured on leaves of detached branches that were placed in a container of water to restore water column during measurement with a PFD of 1500 μmol m^{-2} s^{-1}. Measurements on detached branches of mature trees were chosen because of the difficulties to reach their canopies, and it had been found in our preliminary test that A_{sat} measured on cut twigs were similar to that measured *in situ* in mature individuals with easily-reached canopies performed in species of *S. superba* and *C. sclerophylla* (n = 3 trees for each treatment, Table S2). To reduce the diurnal heterogeneity, A_{sat} measurements were conducted at 9:00–11:30 am on the same day as NSC sample collection in October.

2.3.3. Growth

Before the onset year of the TFE treatment (2012), we marked all the mature trees in TFE and TFE-control plots, and recorded their DBH (diameter at breast height, all trees DBH > 10 cm) in December 2014, 2015 and 2016. Relative DBH increment of all mature tree individuals from the onset of TFE treatment was calculated by [(DBH-DBH_{2012})/DBH_{2012} × 100%] in TFE-control and TFE plots.

2.3.4. Nonstructural carbohydrates

NSC concentrations were measured using a modified phenol-sulfuric method (Chow and Landhäusser, 2004; Zhang et al., 2014). All samples were microwaved at 600 W for 90 s to eliminate enzymatic activity within 4 h after sampling, followed by oven drying for 72 h at 65 °C. Leaf tissues were ground into powders < 0.2 mm particle size with a ball mill (multi-sample tissue homogenizer; Jingxin Industrial Development Co., Ltd., Shanghai, China). Woody tissues were milled with a blade mill prior to ball milling. Soluble sugars were extracted by centrifugation from 60 mg of the ground samples with 10 ml of 80% v/v ethanol for 24 h followed by additional re-extraction with 5 ml of 80% v/v ethanol. The supernatants obtained by two centrifugations were combined together and used for the soluble sugar determination. The ethanol-insoluble residuals were used to extract starch after ethanol evaporation. The starch of the residuals was released by boiling in 10 ml distilled water for 15 min. After cooling to room temperature, the starch was digested with α amylase and further hydrolyzed to glucose by amyloglucosidase. The supernatants were used for determining the concentration of starch. The concentrations of soluble sugars and starch were measured with a spectrophotometer (UV-2550, Shimadzu Corp., Kyoto, Japan) at a wavelength of 490 nm using phenol–sulfuric method based on a glucose standard curve (Palacio et al., 2007). A parallel assay replacing phenol by water was applied to correct the interfering effects on NSC component determination of each sample. The starch concentrations were calculated by multiplying a reference concentration of glucose by the conversion factor of 0.9. Sucrose, fructose and starch were used as standards, and their recoveries were > 95%. One inter-lab standard (peach leaves NIST1547) was also applied in the analyses. The total NSC was calculated as the sum of starch (mg g^{-1}) and soluble sugar (mg g^{-1}) concentrations on a dry matter basis (mg g^{-1} DW).

2.4. Estimating NSC pools at tissues and the whole-tree levels

Biomass of each tissue (leaves, branches, stems and coarse roots) were estimated using allometric equations (Table S3; Gou et al., 2017;

Guisasola, 2014; Lai et al., 2013; Tang et al., 2017; Yang et al., 2010; Zuo et al., 2015). Whole-tree biomass was calculated as the sum of the four tissues. We didn't include fine roots into whole-tree biomass or further NSC pool calculations as there was a lack of equations for fine roots biomass, probably leading to the underestimation of NSC storage in roots. To correct for the biomass differences among trees, we calculated the proportions of total NSC and its component pool sizes relative to whole tree biomass [(concentration × tissue biomass)/whole-tree biomass × 100%]. NSC pools in leaves and coarse roots were determined by tissue biomass and measured NSC concentrations. NSC pools in branches were calculated using the biomass of branch and the NSC concentrations measured from multi-yr-old branches (no significant difference in NSC concentrations of multi-yr-old branches and one-yr-old twigs was observed in our study, $p > 0.05$). To calculate NSC pools in stem, we partitioned the main trunk biomass into three subdivisions (0–3 cm, 3–6 cm and 6 cm-pith stemwood) by calculating the ratio of each subdivision relative to the whole stemwood, and determined stem NSC pools by the sum of NSC storage of these three components. Whole-tree NSC storage was calculated as the sum of NSC storage in each tissue.

2.5. Statistical analyses

Student's *t*-test was used to test the treatment differences for DBH growth in four species, with plots as replicates. Differences in soil moisture, A_{sat} among treatments were also evaluated by Tukey's HSD with plots as replicates. We performed linear regression analyses to evaluate the correlations of NSC concentrations with A_{sat}.

Fixed effects of species, treatments, tissues, sampling time and their interactions on concentrations of NSC and its components in each tree life stage were tested by the repeated measures linear mixed-effects models (LME) fit by maximum likelihood using *lme* function of *NLME* package in R v. 3.5.1. Each plot was considered as a random effect, and mean tree biomass of mature trees or mean stem diameter of seedlings in each plot ware used as covariates. For mature trees, we also used a LME model to test those fixed effects on total NSC, sugars, and starch pools in leaves, branches, stems and coarse roots (Table S4). Data was transformed to obtain the normality of residuals. Differences in NSC (and its components) concentrations and pool sizes among the TFE-control plots, ambient and the TFE plots were tested using Tukey's HSD. TFE effects on NSC across sampling periods were defined as the change in NSC (by tissue) from the TFE treatment relative to the TFE-control treatment and its difference from zero was tested by *t*-test. All data analyses were conducted with the software R v. 3.5.1 (R Core Team, 2018).

3. Results

3.1. Soil volumetric moisture content

During the monsoon period (July to September), air temperature and vapor pressure deficit (VPD) were relatively high, and the soil volumetric moisture content (VWC%) fluctuated (Figs. 1, S2). No difference in VWC% was found between TFE-control plots and ambient plots, while the VWC% in drought plots was significantly lower than those in control and ambient plots at soil depths from 5 cm to 75 cm. Averaged across all depths, VWC% in throughfall exclusion experiment (TFE) treatment, TFE- control and ambient plots were 14.32 ± 0.19%, 22.12 ± 0.16%, and 22.43 ± 0.82%, respectively. Compared to the mean VWC% in control plots, that in TFE reduced 37.3 ± 1.2%, 27.5 ± 1.1%, 42.1 ± 0.7%, 34.9 ± 0.6% and 34.2 ± 0.9%, respectively, at depth of 5 cm, 15 cm, 30 cm, 50 cm and 75 cm ($p < 0.001$, Fig. 1).

3.2. Photosynthesis and growth

Light-saturated photosynthesis (A_{sat}) differed among species, with the lowest A_{sat} occurring in *C. carlesii* ($p < 0.001$, Fig. 2). TFE did not change A_{sat} in mature trees, while it did cause a significant decrease of A_{sat} in seedlings of *C. carlesii* and *C. sclerophylla* and a slight decrease in seedlings of *L. glaber* (45.6 ± 2.0%, 36.1 ± 2.0%, 20.6 ± 2.1%, respectively) (Fig. 2b–d).

During the 4-yr TFE treatment, the mature trees of *S. superba* and *C. carlesii* grew faster than those of *L. glaber* and *C. sclerophylla*, and the reduced throughfall showed no significant impact on tree growth in mature trees of all four species ($p > 0.05$, Fig. 3).

3.3. Drought effect on NSC storage in mature trees and seedlings

There was no significant difference in concentrations of NSC and its fractions between TFE-control and ambient plots in mature trees ($p > 0.05$; Figs. 4, S3, S4; Table S4). The TFE treatment only showed significant impacts on NSC and sugar concentrations of 0–3 cm stemwood in *C. carlesii* in January, while no significant change occurred in other tissues of other three species (Figs. S5, S6).

For seedlings, however, TFE treatment had a significant effect on NSC and its component concentrations in foliage (Table 2). Total NSC and soluble sugars of leaves significantly decreased in *S. superba* in August and January, and those of 1-yr-old branches also decreased for all sample dates (Figs. 5a, e, 6a, e). In seedlings of *C. carlesii*, total NSC and soluble sugars in foliage only decreased in October under TFE treatment (Figs. 5c, g, 6c, g). Averaged across all sampling times, TFE treatment significantly decreased total NSC concentrations in seedling leaves of *S. superba* and *C. sclerophylla* by 18.64 ± 4.29% and 8.48 ± 3.87%, respectively, and in branches by 28.50 ± 1.70% and 9.78 ± 2.05%, respectively (Fig. 7a, e, d, h). The decreased trends were also observed in the seedlings of *C. carlesii*, although it was not statistically significant (Fig. 7c, g). The observed decreases in total NSC concentrations were mainly from decreases in soluble sugars, as starch showed no change in seedlings of these species (Fig. 7). However, in seedlings of *L. glaber*, soluble sugars and total NSC in leaves increased slightly and starch in 1-yr-old twigs increased significantly in August (Fig. 5b, f, 6j, 7b).

4. Discussion

Our throughfall exclusion experiment (TFE) tested the differential responses of NSC storage to drought in mature trees and understory seedlings under field conditions. Our results showed that NSC significantly decreased in foliage of seedlings of *S. superba* and *C. carlesii* by drought but was maintained in all mature trees under TFE treatments at all tissues (Figs. 4–6), partially supporting the hypothesis that NSC in seedlings declined more than in mature trees under drought. Whole-tree NSC storage of mature trees was also stable under drought, although it exhibited significant variations in tissues and seasons as temperate species (Furze et al., 2019). Meanwhile, the NSC responses to drought in seedlings were species-specific, as the NSC decreased trends shown in foliage of the other three species were not observed in the seedlings of *L. glaber*, of which soluble sugars and starch were maintained or even slightly increased (Fig. 7). These results indicate the different fate of carbohydrate reserves in seedlings and mature trees responding to drought (Hartmann et al., 2018).

4.1. More drought-induced decline in NSC in seedlings than mature trees

Our observation that NSC maintained at tissues and whole-tree levels of mature trees but decreased in seedling foliage of three species, indicates the higher sensitivity of C storage to drought in understory seedlings than mature trees (Figs. 4–7; Table 2). These differences might largely result from the different drought sensitivity of

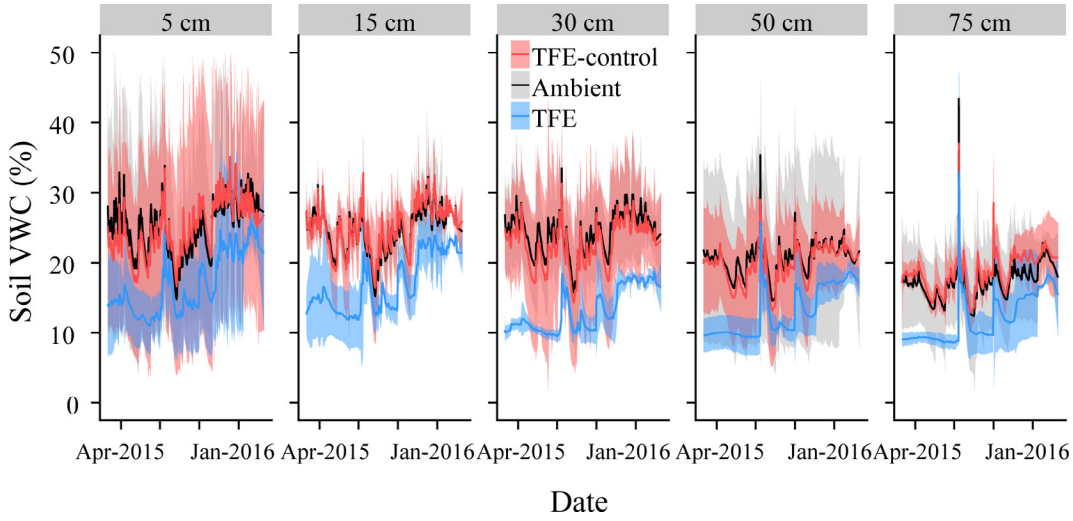

Fig. 1. Daily mean volumetric soil water content (VWC, %) recorded at depths of 5 cm, 15 cm, 30 cm, 50 cm and 75 cm from March 2015 to February 2016. Values under each treatment were calculated by averaging the daily means of measurements from the three replicate plots. Three sensors were applied and averaged per soil depth for each plot. Shaded areas represent 95% confidence intervals of the daily means.

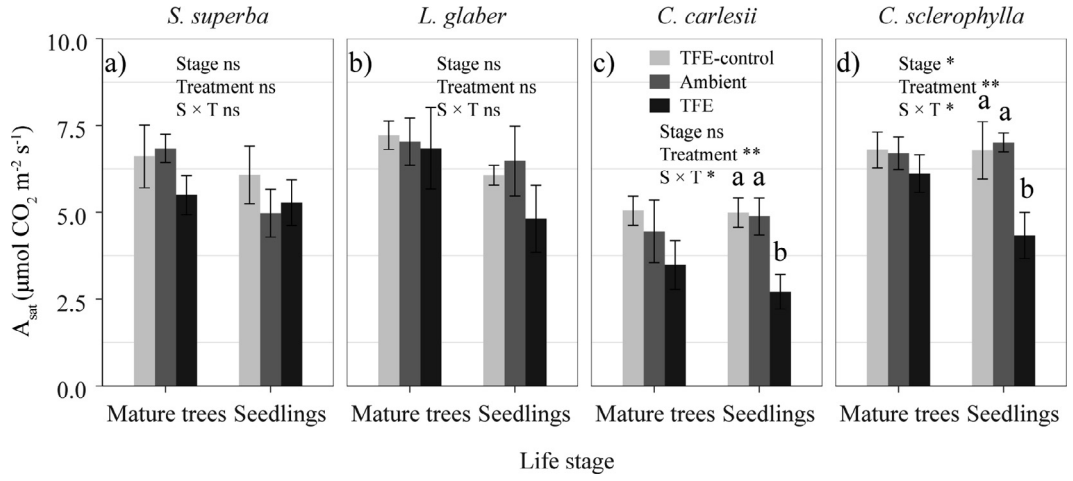

Fig. 2. Net photosynthesis rate at saturated light intensity (A_{sat}) in mature trees and seedlings of four species measured in throughfall exclusion (TFE), TFE-control treatments and ambient plots in October 2015. Values are means ± standard errors (n = 3 plots, measurements on two tree individuals within a plot were averaged for each species × treatment × size combination). The effect of life stage, treatment and their interaction (S × T) for each species were shown (ns, $p > 0.05$; *, $p < 0.05$; **, $p < 0.01$; ***, $p < 0.001$). Different lower cases represent significant differences among treatments at $\alpha = 0.05$.

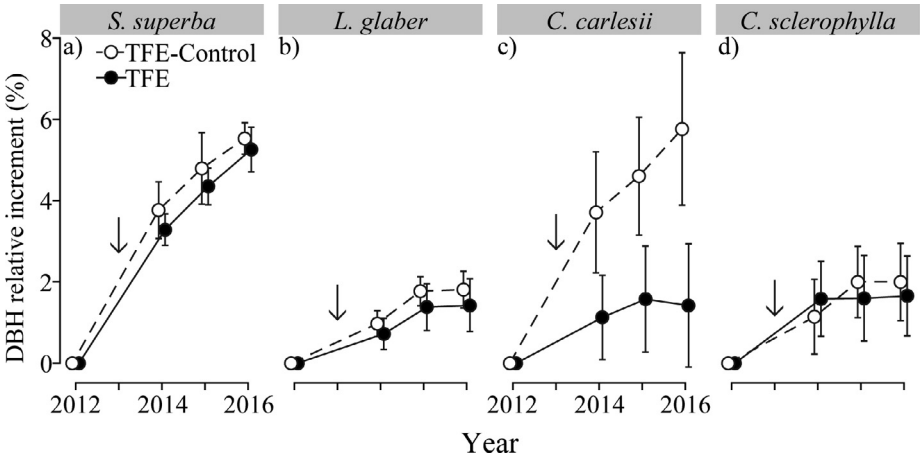

Fig. 3. Cumulative relative increment of diameter at breast height (DBH) from the year of 2012 in mature trees of four species in throughfall exclusion (TFE) and TFE-control plots. The onset year of TFE (2013) is marked in arrow. Values are means ± standard errors (n = 3 plots, all trees DBH > 10 cm for each species were averaged). Tree DBH relative increment between treatments were not significantly different in each year for all species (*t* test, $p > 0.05$).

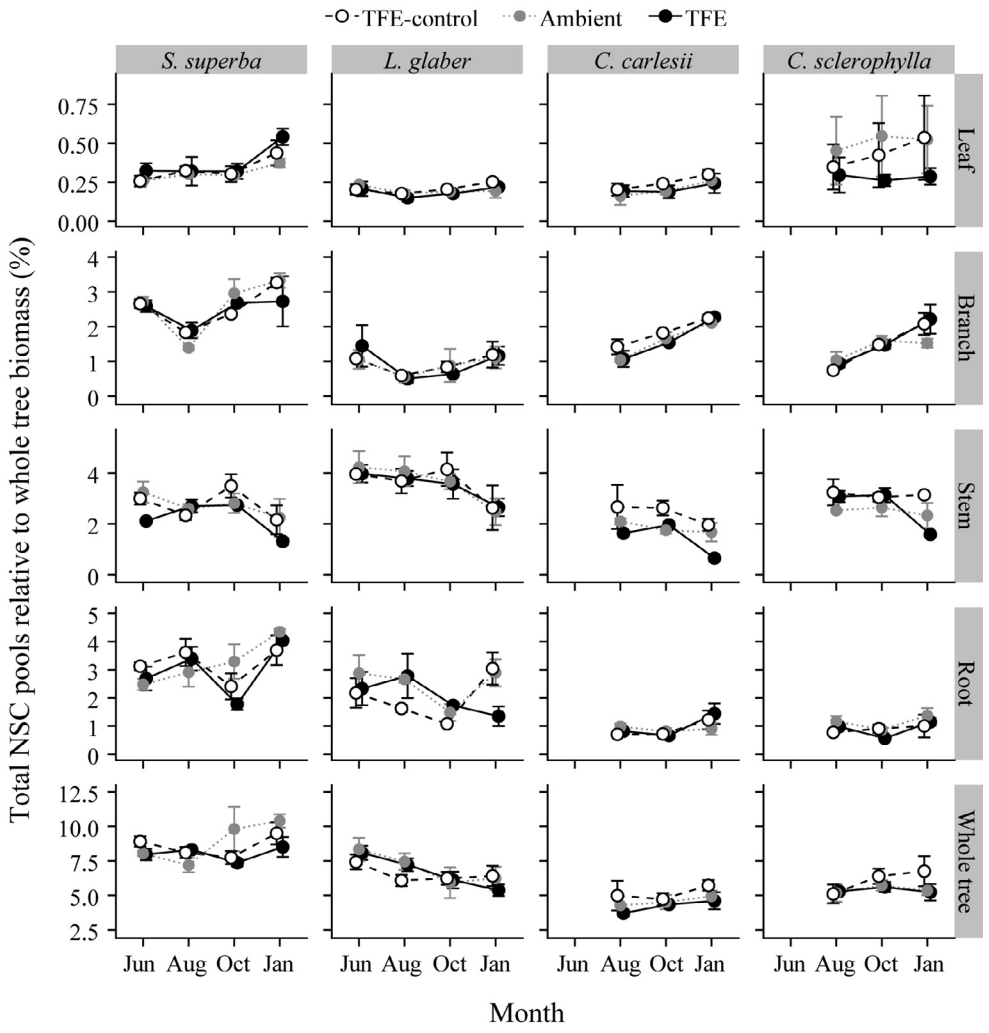

Fig. 4. Total nonstructural carbohydrates (NSC) in leaves, branches, stems, coarse roots and whole-tree levels for mature trees of four species in throughfall exclusion (TFE), TFE-control treatments and ambient plots throughout the June 2015 to January 2016. Values are means ± standard errors (n = 3 plots, measurements on two tree individuals within a plot were averaged for each species × treatment combination). Total NSC pools among treatments were not significantly different at tissues or the whole-tree levels for all species and sampling time (Tukey's HSD, $p > 0.05$).

Table 2
F-value of repeated measures linear mixed-effects models test for the effect of month, species, tissues and treatment on NSC concentrations and its components ($mg \cdot g^{-1}DW$) in mature trees and seedlings of four species. Significant effect is shown in bold. For mature trees, mean tree biomass of each species in each plot was included as a covariate. For seedlings, mean stem diameter of each species in each plot was included as the covariate.

Fixed factors	Mature trees			Seedlings		
	NSC (*Sqrt(x)*)	Sugars (*Sqrt(x)*)	Starch (*Log(x + 1)*)	NSC (*Sqrt(x)*)	Sugars (*Sqrt(x)*)	Starch (*x*)
Month	**8.26*****	**10.96*****	**11.12*****	**182.79*****	**153.10*****	**66.64*****
Species	**85.24*****	**93.60*****	**6.69*****	**104.26*****	**104.18*****	**12.48*****
Tissues	**183.52*****	**205.56*****	**103.07*****	**100.52*****	**108.85*****	**7.70****
Treatment	0.01	0.09	0.24	**8.63*****	**15.41*****	1.01
Month × Species	1.03	**2.25***	1.04	**7.34*****	**7.13*****	**7.03*****
Month × Tissue	**27.66*****	**20.45*****	**31.82*****	**3.53***	**6.43****	**34.55*****
Month × Treatment	0.86	1.62	1.31	**3.91****	2.10	**3.01***
Species × Tissue	**7.09*****	**9.19*****	**2.18****	0.65	0.92	1.04
Species × Treatment	0.25	0.50	0.96	**10.30*****	**9.16*****	**3.41****
Tissue × Treatment	1.52	0.82	**1.92***	2.40	3.04	0.27
Month × Species × Tissue	1.31	**1.57***	1.23	1.64	1.77	1.63
Month × Species × Treatment	0.64	0.88	0.35	**3.02*****	2.86	1.83
Month × Tissue × Treatment	**1.66***	1.33	1.16	0.71	0.32	1.96
Species × Tissue × Treatment	0.78	0.71	1.01	0.88	0.66	0.74
Month × Species × Tissue × Treatment	0.88	0.97	0.92	0.62	0.27	1.33

* $p < 0.05$.
** $p < 0.01$.
*** $p < 0.001$.

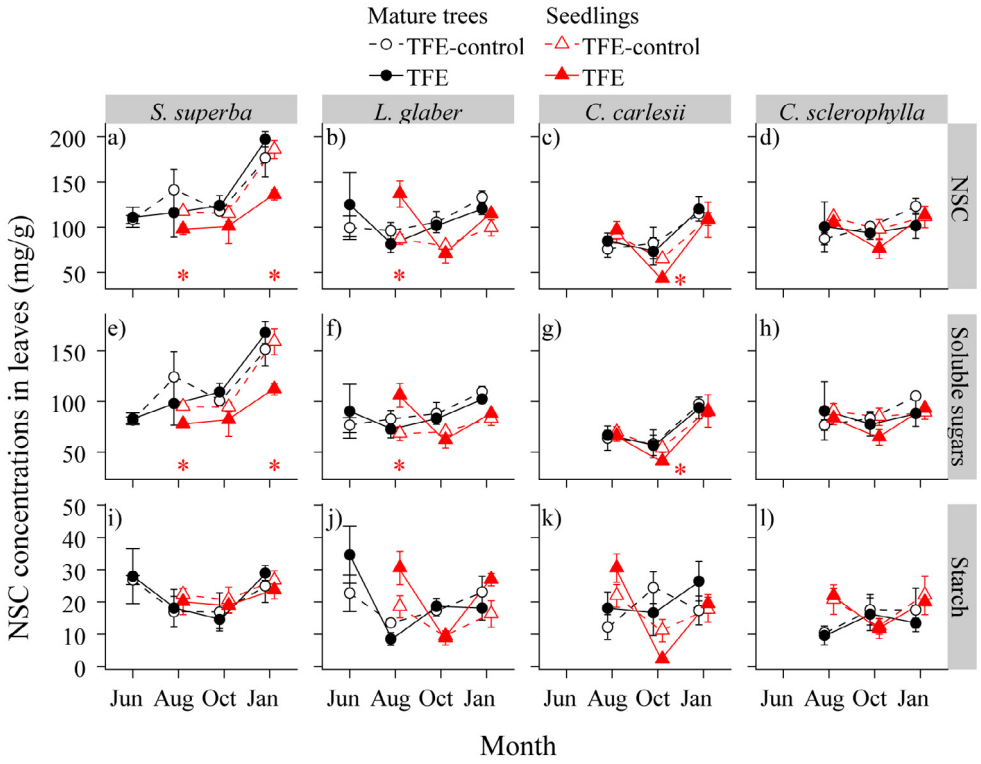

Fig. 5. Concentrations of nonstructural carbohydrates (NSC, a–d), soluble sugars (e–h) and starch (i–l) in leaves of mature trees (circles) and seedlings (triangles) for four species under throughfall exclusion (TFE, black solid circles and red solid triangles), and TFE-control treatments (open circles and open triangles) throughout the June 2015 to January 2016. Values are means ± standard errors (n = 3 plots, measurements on two tree individuals within a plot were averaged for each species × treatment × size combination). The red asterisk denotes the values of the seedlings in TFE are significantly different from those under TFE-control/ambient treatments (Tukey's HSD, $p < 0.05$). The values of ambient plots were not shown as they were not significantly different from that of TFE-control treatment ($p > 0.05$, Table S5).

photosynthesis in trees of two life stages, as photosynthesis showed significant decreases in seedlings (especially in *C. carlesii* and *C. sclerophylla*) but maintained in mature trees under the TFE treatment (Fig. 2). Our findings were in line with a previous study, where photosynthesis in seedlings of *Quercus rubra* decreased more severely than that in mature trees in a drought year (Cavender-Bares and Bazzaz, 2000). The reduction of newly assimilated C would lead to a fast decline of foliage carbon reserve due to the relatively small NSC pools (Niinemets, 2010). For mature trees, however, their stable photosynthesis and homeostatic C storage indicate higher stabilities under drought. These contrasted photosynthetic performances under drought in two life stages may be resulted from the ontogenetic differences in drought response strategy like stomatal regulation abilities (Cavender-Bares and Bazzaz, 2000), but may be also associated with the degree of drought stress on trees in canopy and understory (Smith et al., 2019).

Further evidence of the consistent lack of precipitation removal

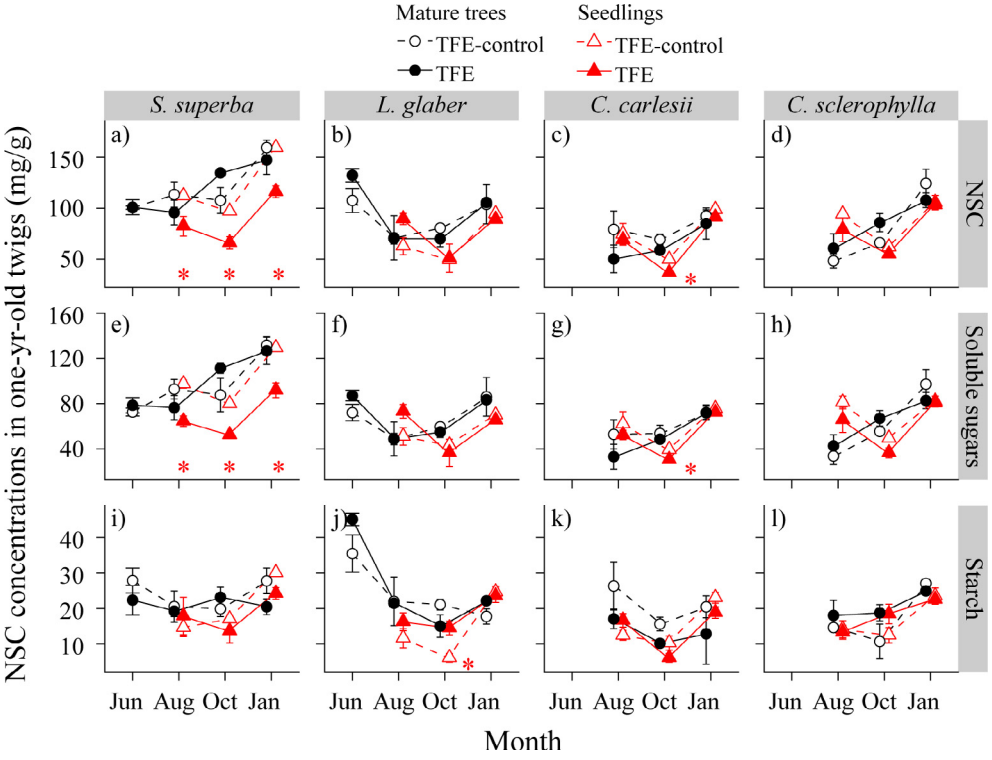

Fig. 6. Concentrations of nonstructural carbohydrates (NSC, a–d), soluble sugars (e–h) and starch (i–l) in one-yr-old twigs of mature trees (circles) and seedlings (triangles) for four species under throughfall exclusion (TFE, black solid circles and red solid triangles), and TFE-control treatments (open circles and open triangles) throughout the June 2015 to January 2016. Values are means ± standard errors (n = 3 plots, measurements on two tree individuals within a plot were averaged for each species × treatment × size combination). The red asterisk denotes the values of the seedlings in TFE are significantly different from those under TFE-control/ambient treatments (Tukey's HSD, $p < 0.05$). The values of ambient plots were not shown as they were not significantly different from that of TFE-control treatment ($p > 0.05$, Table S5).

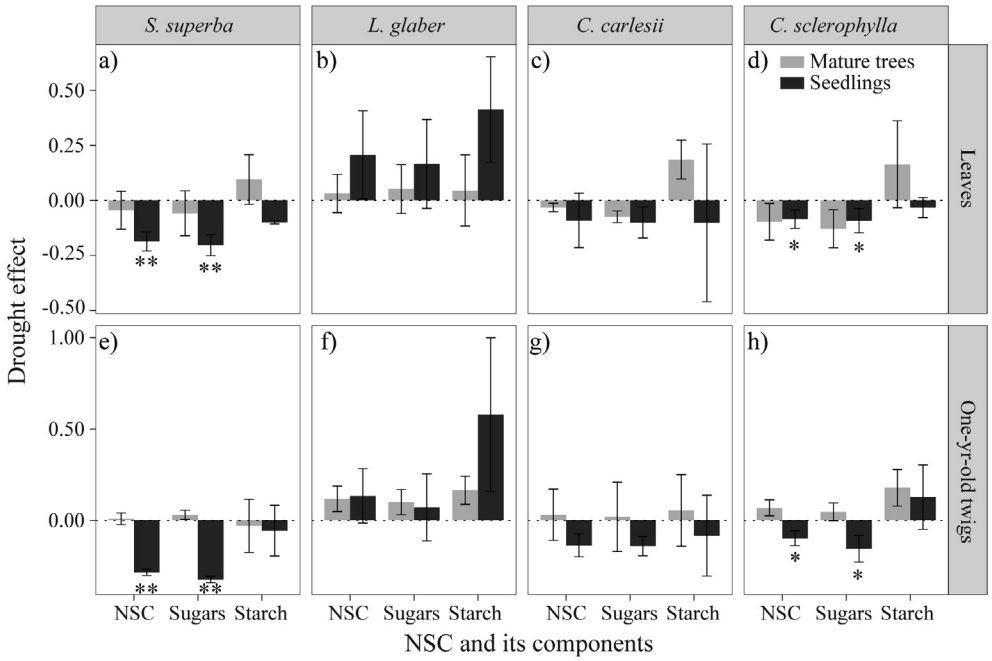

Fig. 7. Drought effect [(TFE-TFEcontrol)/TFEcontrol] on NSC and its components in mature trees and seedlings. Values are means ± standard errors across four sampling times (June, August, October of 2015 and January of 2016). The horizontal dotted line was drawn at the Drought effect = 0. Asterisks represent the significant differences between drought effect and zero (*, $p < 0.05$; **, $p < 0.01$).

effect on growth rates during the 3-year TFE treatment (Fig. 3) also suggests that mature trees have good persistence and higher avoidance of future drought than understory seedlings. This is conflicted with some recent reports that larger trees were more susceptible to drought and experienced higher rates of mortality (Bennett et al., 2015; Stovall et al., 2019). The longer xylem hydraulic path and exposure to more arid canopy environments in large trees might contribute to their vulnerabilities to drought compared to those in small trees (Olson et al., 2018; Rowland et al., 2015). However, the other evidences have also shown that larger trees are more resilient to drought (Giardina et al., 2018; Smith et al., 2019). We speculated that the homeostatic tree physiology in mature trees cannot be explained by the drought acclimation because drought did not affect tree growth rates since the TFE initiation (Fig. 3). In contrast, the increasing uptake of deeper soil water due to extensive root systems in mature trees can make them have greater water storage capacity, contributing to their stronger avoidance of drought stress (McDowell et al., 2019; Yang et al., 2015). Indeed, the use of deep soil water can help trees cope with short-time or mild drought, although the larger trees are thought less tolerant of water stress (Brum et al., 2019). This is supported by the evidence that understory seedlings exhibited higher sensitivity in radial growth, water potential, and leaf area to environmental stresses than mature trees (Cavender-Bares and Bazzaz, 2000; Oberhuber et al., 2015; Smith et al., 2019). It is worthy to note that this difference in tree life stages may be confounded with the environmental factors (e.g., light, temperature, air humidity). However, we did not try to disentangle the environmental effects from tree size one because it would be more representative in the responses of mature trees and understory seedlings to natural drought, offering potential to improve the understanding of forest succession under drought in the future.

4.2. Variable sugar but maintained starch in understory seedlings under drought

The two primary components of the measured NSC, soluble sugars and starch, have different physiological functions. Soluble sugars comprise a short-term C pool for ephemeral demands, while starch often functions as a storage compound for future needs (Dietze et al. 2014; Martínez-Vilalta et al., 2016). Previous studies have found that soluble sugars tended to maintain or even increase at the expense of starch depletion in potted seedlings under drought (Maguire and Kobe, 2015; Mitchell et al., 2013; Rodríguez-Calcerrada et al., 2017). These results are generally assumed to be associated with the function of soluble sugars in osmotic regulation and turgor maintenance (Martínez-Vilalta et al., 2016; O'Brien et al., 2014). However, we found drought reduced concentrations of soluble sugars but did not change starch concentrations in the understory seedlings (Figs. 5–7). This was consistent with some studies on seedlings under drying-watering cycles (Duan et al., 2014; Hartmann et al., 2013; O'Brien et al., 2015) and with those exposed to a combination of drought and shading (Maguire and Kobe, 2015; Piper and Fajardo, 2016). This discrepancy in responses of NSC components to drought suggests the greater complexity in physiological responses to drought in understory seedlings of natural forests compared to that on potted seedlings.

The variable sugar concentrations but unchanged starch concentrations in seedling foliage induced by drought may be associated with the survival strategies under the understory environment with low light irradiation, relative higher humidity, diverse disturbance, and high competition (Kobe, 1997). On one hand, the low-light understories may reduce aboveground sink strength of understory seedlings and increase C investment to below-ground growth/metabolisms to gain more water/nutrient resources when the upper soil layer becomes dry (Markesteijn and Poorter, 2009). Thus, lower soluble sugars were often found under the reduced metabolic demands in foliage induced by mild drought. On the other hand, the maintenance of starch at a certain level would contribute to the rapid recovery after short disturbance in the field understory environment (such as variable water availability, stem damage, herbivory and pathogens infection), as starch always acts as a carbon reservoir for the future use and may support tissue regrowth (Martínez-Vilalta et al., 2016; Trugman et al., 2018). Under extreme drought, however, starch can be depleted, while soluble sugar might be maintained above a critical threshold for the function in osmotic regulation (Martínez-Vilalta et al., 2016; Wiley et al., 2019). Therefore, further studies on the variations in NSC components with drought severity are needed to understand C utilization strategies of understory seedlings in response to drought. Moreover, to protect the seedlings at the site, our sampling was limited to the seedling foliage. We did not detect the belowground NSC dynamics of seedlings, which plays a critical role in tree survival under drought (Hagedorn et al. 2016). More studies on belowground NSC storage of field forests are critical to better

probe the mechanisms of trees C allocation under adverse environment.

4.3. NSC responses to drought are species-specific in understory seedlings

Both soluble sugar and starch concentrations showed slight increases for the seedlings of *L. glaber* as opposed to the other three species, indicating species-specific NSC responses to drought (Fig. 7). These species-specific NSC responses are in line with other studies, where drought-induced changes in NSC changed in trees with different drought response strategies (Lloret et al., 2018; Mitchell et al., 2014; Piper, 2011). Specifically, NSC decreased in the relatively more drought-susceptible species but increased in the more drought-resistant species (Piper, 2011). Trees with higher embolism resistance are less likely to deplete NSC storage at drought-induced mortality (Adams et al., 2017). Among the four species, *L. glaber* has the highest dehydration tolerance and the maximum xylem conductance (Kröber et al., 2015; Zhang et al., 2012), suggesting that the uniqueness of *L. glaber* may be due to high hydraulic resistance. Thus, the understanding of tree NSC responses to drought should be always coupled with the hydraulic traits in trees (McDowell et al., 2011a). Indeed, the variable NSC responses as well as the different drought resistance in coexisting seedlings suggest functional diversity in forests that would enhance forest resilience to drought (De la Riva et al., 2017), and have great implications for forest succession and vegetation dynamics under future extreme climatic change.

4.4. Implications for the future experiments and modeling

Despite the importance of NSCs to tree metabolism and survival under drought, we have a limited understanding of how NSC regulation varies from seedlings to mature trees (Hartmann et al., 2018). Our TFE study, for the first time to best of our knowledge, provides evidence of different drought sensitivity of NSC storage in tree life stages. Although our study highlights the differential NSC responses from seedlings to mature forests, more studies are necessary. First, complete carbon budgets of field-grown small and large trees are needed to understand carbon allocation as they vary with tree life stages. Our results are indicative of different behavior in NSC concentrations in relation to drought in two life stages. Through complete carbon budgets including photosynthesis, tissue growth, respiration and C storage we can better assess the mechanisms leading to these patterns. Meanwhile, incorporating carbon budgets and other physiological indicators (e.g., hydraulics and morphology, root depth) into future studies may provide insights into the key mechanisms driving trees' survival, competition, forest composition and regeneration. Second, the responses of soluble sugars to drought in understory seedlings were inconsistent with potted seedlings in other studies. Most of current controlled experiments on potted seedlings only focused on single-factor and short-time effects, providing the potential to easily understand the physiological mechanisms. However, the physiology for field-growing seedlings may be different to adapt to inconstant environment and kinds of understory disturbance. Thus further studies on seedlings with multi-disturbance should be conducted to better understand natural forest responses to future extreme drought. Third, seedlings are often regarded as small trees and their physiological mechanisms are used for simulating C allocation in mature trees. However, the observed stage-dependent differences in NSC storage sensitivities and drought-resistance suggest the extrapolation from seedlings to mature trees are questionable. Linking continuous assessments of carbon fluxes and pools on seedlings with the discrete observation on mature trees and flux measurements at ecosystem scale is a realistic way to provide better representations of C allocation and storage in vegetation models (Hartmann et al., 2018). Therefore, the stage-related differences and interactions are required to be considered in future vegetation models to forecast the forest dynamics under climate change.

5. Conclusions

Our TFE study indicates intrinsic variations in drought sensitivities of carbohydrates storage to drought between mature trees and understory seedlings, providing insights to the stage-dependent C storage traits. Seedlings are more likely to suffer from the changes in NSC and soluble sugars under drought while mature trees tend to maintain NSC, suggesting different trade-offs between C accumulation and consumption in two life stages under drought. It deserves further study to examine how ontogenetic and environmental differences may affect NSC regulation in drought-induced mortality of trees in relation to different life stages on both canopy dominant and understory trees. Therefore, the characteristic of carbon allocation and storage in tree life stages under drought would be incorporated into vegetation models to gain the key constraints of upscaling and better predict vegetation dynamics in natural forests.

CRediT authorship contribution statement

Peipei Zhang: Conceptualization, Formal analysis, Investigation, Visualization, Writing - original draft. **Xuhui Zhou:** Funding acquisition, Writing - review & editing. **Yuling Fu:** Project administration, Supervision. **Junjiong Shao:** Methodology, Writing - review & editing. **Lingyan Zhou:** Writing - review & editing. **Songsong Li:** Investigation. **Guiyao Zhou:** Investigation, Writing - review & editing. **Zhenhong Hu:** Investigation. **Jiaqi Hu:** Investigation, Visualization. **Shahla Hosseini Bai:** Writing - review & editing. **Nate G. McDowell:** Writing - review & editing.

Acknowledgements

The authors thank the editor and three anonymous reviewers for their insightful comments and suggestions. The authors thank Guodong Zhang and Liling Jiang for their help with field work. Many thanks to Shasha Li and Sheng Gao for their assistance with sample preparation. This study was financially supported by the National Natural Science Foundation of China (Grant No. 31930072, 31600387, 31770559) and the 'Thousand Young Talents' Program in China. NGM was supported by the Pacific Northwest National Laboratories LDRD program and the Department of Energy's Next-Generation Ecosystem Experiment (NGEE)-Tropics.

Appendix A. Supplementary material

Supplementary data to this article can be found online at https://doi.org/10.1016/j.foreco.2020.118159.

References

Adams, H.D., Collins, A.D., Briggs, S.P., Vennetier, M., Dickman, L.T., Sevanto, S.A., Garcia-Forner, N., Powers, H.H., McDowell, N.G., 2015. Experimental drought and heat can delay phenological development and reduce foliar and shoot growth in semiarid trees. Glob. Change Biol. 21, 4210–4220. https://doi.org/10.1111/gcb.13030.

Adams, H.D., Zeppel, M.J.B., Anderegg, W.R.L., Hartmann, H., Landhausser, S.M., Tissue, D.T., Huxman, T.E., Hudson, P.J., Franz, T.E., Allen, C.D., Anderegg, L.D.L., Barron-Gafford, G.A., Beerling, D.J., Breshears, D.D., Brodribb, T.J., Bugmann, H., Cobb, R.C., Collins, A.D., Dickman, L.T., Duan, H., Ewers, B.E., Galiano, L., Galvez, D.A., Garcia-Forner, N., Gaylord, M.L., Germino, M.J., Gessler, A., Hacke, U.G., Hakamada, R., Hector, A., Jenkins, M.W., Kane, J.M., Kolb, T.E., Law, D.J., Lewis, J.D., Limousin, J.-M., Love, D.M., Macalady, A.K., Martinez-Vilalta, J., Mencuccini, M., Mitchell, P.J., Muss, J.D., O'Brien, M.J., O'Grady, A.P., Pangle, R.E., Pinkard, E.A., Piper, F.I., Plaut, J.A., Pockman, W.T., Quirk, J., Reinhardt, K., Ripullone, F., Ryan, M.G., Sala, A., Sevanto, S., Sperry, J.S., Vargas, R., Vennetier, M., Way, D.A., Xu, C., Yepez, E.A., McDowell, N.G., 2017. A multi-species synthesis of physiological mechanisms in drought-induced tree mortality. Nat. Ecol. Evol. 1, 1285–1291. https://doi.org/10.1038/s41559-017-0248-x.

Allen, C.D., Breshears, D.D., McDowell, N.G., 2015. On underestimation of global vulnerability to tree mortality and forest die-off from hotter drought in the Anthropocene. Ecosphere 6, art129. https://doi.org/10.1890/ES15-00203.1.

Allen, C.D., Macalady, A.K., Chenchouni, H., Bachelet, D., McDowell, N., Vennetier, M.,

Kitzberger, T., Rigling, A., Breshears, D.D., Hogg, E.H. (Ted), Gonzalez, P., Fensham, R., Zhang, Z., Castro, J., Demidova, N., Lim, J.-H., Allard, G., Running, S.W., Semerci, A., Cobb, N., 2010. A global overview of drought and heat-induced tree mortality reveals emerging climate change risks for forests. For. Ecol. Manag., Adaptation of Forests and Forest Management to Changing ClimateSelected papers from the conference on "Adaptation of Forests and Forest Management to Changing Climate with Emphasis on Forest Health: A Review of Science, Policies and Practices", Umeå, Sweden, August 25-28, 2008. 259, 660–684. 10.1016/j.foreco.2009.09.001.

Anderegg, W.R.L., Kane, J.M., Anderegg, L.D.L., 2013. Consequences of widespread tree mortality triggered by drought and temperature stress. Nat. Clim. Change 3, 30–36. https://doi.org/10.1038/nclimate1635.

Augspurger, C.K., Bartlett, E.A., 2003. Differences in leaf phenology between juvenile and adult trees in a temperate deciduous forest. Tree Physiol. 23, 517–525. https://doi.org/10.1093/treephys/23.8.517.

Baber, O., Slot, M., Celis, G., Kitajima, K., 2014. Diel patterns of leaf carbohydrate concentrations differ between seedlings and mature trees of two sympatric oak species. Bot.-Bot. 92, 535–540. https://doi.org/10.1139/cjb-2014-0032.

Bennett, A.C., McDowell, N.G., Allen, C.D., Anderson-Teixeira, K.J., 2015. Larger trees suffer most during drought in forests worldwide. Nat. Plants 1, 15139. https://doi.org/10.1038/nplants.2015.139.

Brum, M., Vadeboncoeur, M.A., Ivanov, V., Asbjornsen, H., Saleska, S., Alves, L.F., Penha, D., Dias, J.D., Aragão, L.E.O.C., Barros, F., Bittencourt, P., Pereira, L., Oliveira, R.S., 2019. Hydrological niche segregation defines forest structure and drought tolerance strategies in a seasonal Amazon forest. J. Ecol. 107, 318–333. https://doi.org/10.1111/1365-2745.13022.

Cavender-Bares, J., Bazzaz, F.A., 2000. Changes in drought response strategies with ontogeny in Quercus rubra: implications for scaling from seedlings to mature trees. Oecologia 124, 8–18. https://doi.org/10.1007/PL00008865.

Chapin, F.S., Schulze, E.-D., Mooney, H.A., 1990. The Ecology and Economics of Storage in Plants. Annu. Rev. Ecol. Syst. 21, 423–447.

Chow, P.S., Landhäusser, S.M., 2004. A method for routine measurements of total sugar and starch content in woody plant tissues. Tree Physiol. 24, 1129–1136. https://doi.org/10.1093/treephys/24.10.1129.

de la Riva, E.G., Lloret, F., Pérez-Ramos, I.M., Marañón, T., Saura-Mas, S., Díaz-Delgado, R., Villar, R., 2017. The importance of functional diversity in the stability of Mediterranean shrubland communities after the impact of extreme climatic events. J. Plant Ecol. 10, 281–293. https://doi.org/10.1093/jpe/rtw027.

Dickman, L.T., McDowell, N.G., Grossiord, C., Collins, A.D., Wolfe, B.T., Detto, M., Wright, S.J., Medina-Vega, J.A., Goodsman, D., Rogers, A., Serbin, S.P., Wu, J., Ely, K.S., Michaletz, S.T., Xu, C., Kueppers, L., Chambers, J.Q., 2019. Homoeostatic maintenance of nonstructural carbohydrates during the 2015–2016 El Niño drought across a tropical forest precipitation gradient. Plant Cell Environ. 42, 1705–1714. https://doi.org/10.1111/pce.13501.

Dickman, L.T., Mcdowell, N.G., Sevanto, S., Pangle, R.E., Pockman, W.T., 2015. Carbohydrate dynamics and mortality in a piñon-juniper woodland under three future precipitation scenarios. Plant Cell Environ. 38, 729–739. https://doi.org/10.1111/pce.12441.

Dietze, M.C., Sala, A., Carbone, M.S., Czimczik, C.I., Mantooth, J.A., Richardson, A.D., Vargas, R., 2014. Nonstructural Carbon in Woody Plants. Annu. Rev. Plant Biol. 65, 667–687. https://doi.org/10.1146/annurev-arplant-050213-040054.

Duan, H., Duursma, R.A., Huang, G., Smith, R.A., Choat, B., O'Grady, A.P., Tissue, D.T., 2014. Elevated [CO2] does not ameliorate the negative effects of elevated temperature on drought-induced mortality in Eucalyptus radiata seedlings. Plant Cell Environ. 37, 1598–1613. https://doi.org/10.1111/pce.12260.

Furze, M.E., Huggett, B.A., Aubrecht, D.M., Stolz, C.D., Carbone, M.S., Richardson, A.D., 2019. Whole-tree nonstructural carbohydrate storage and seasonal dynamics in five temperate species. New Phytol. 221, 1466–1477. https://doi.org/10.1111/nph.15462.

Galvez, D.A., Landhäusser, S.M., Tyree, M.T., 2011. Root carbon reserve dynamics in aspen seedlings: does simulated drought induce reserve limitation? Tree Physiol. 31, 250–257. https://doi.org/10.1093/treephys/tpr012.

Giardina, F., Konings, A.G., Kennedy, D., Alemohammad, S.H., Oliveira, R.S., Uriarte, M., Gentine, P., 2018. Tall Amazonian forests are less sensitive to precipitation variability. Nat. Geosci. 11, 405–409. https://doi.org/10.1038/s41561-018-0133-5.

Gou, M., Xiang, W., Song, T., Lei, P., Zhang, S., Ouyang, S., Zeng, Y., Deng, X., Fang, X., Wang, K., 2017. Allometric equations for applying plot inventory and remote sensing data to assess coarse root biomass energy in subtropical forests. BioEnergy Res. 10, 536–546. https://doi.org/10.1007/s12155-017-9820-0.

Gruber, A., Pirkebner, D., Florian, C., Oberhuber, W., 2012. No evidence for depletion of carbohydrate pools in Scots pine (Pinus sylvestris L.) under drought stress. Plant Biol. 14, 142–148. https://doi.org/10.1111/j.1438-8677.2011.00467.x.

Guisasola, R., 2014. Allometric Biomass Equations and Crown Architecture in Mixed-species Forests of Subtropical China. Albert-Ludwigs Univ. Freibg., Freibg. Ger.

Hagedorn, F., Joseph, J., Peter, M., Luster, J., Pritsch, K., Geppert, U., Kerner, R., Molinier, V., Egli, S., Schaub, M., Liu, J.-F., Li, M., Sever, K., Weiler, M., Siegwolf, R.T.W., Gessler, A., Arend, M., 2016. Recovery of trees from drought depends on belowground sink control. Nat. Plants 2, 16111. https://doi.org/10.1038/NPLANTS.2016.111.

Hartmann, D.L., 2016. Global Physical Climatology, second ed. Elsevier, Amsterdam Boston Heidelberg.

Hartmann, H., Adams, H.D., Anderegg, W.R.L., Jansen, S., Zeppel, M.J.B., 2015. Research frontiers in drought-induced tree mortality: crossing scales and disciplines. New Phytol. 205, 965–969. https://doi.org/10.1111/nph.13246.

Hartmann, H., Adams, H.D., Hammond, W.M., Hoch, G., Landhäusser, S.M., Wiley, E., Zaehle, S., 2018. Identifying differences in carbohydrate dynamics of seedlings and mature trees to improve carbon allocation in models for trees and forests. Environ. Exp. Bot. 152, 7–18. https://doi.org/10.1016/j.envexpbot.2018.03.011.

Hartmann, H., Ziegler, W., Trumbore, S., 2013. Lethal drought leads to reduction in nonstructural carbohydrates in Norway spruce tree roots but not in the canopy. Funct. Ecol. 27, 413–427. https://doi.org/10.1111/1365-2435.12046.

He, J.-S., Zhang, Q.-B., Bazzaz, F.A., 2005. Differential drought responses between saplings and adult trees in four co-occurring species of New England. Trees 19, 442–450. https://doi.org/10.1007/s00468-004-0403-2.

Hoch, G., 2015. Carbon reserves as indicators for carbon limitation in trees. In: Progress in Botany, Progress in Botany. Springer, Cham, pp. 321–346. 10.1007/978-3-319-08807-5_13.

IPCC, 2014. Climate Change 2014: Synthesis Report. Contribution of Working Groups I, II and III to the Fifth Assessment Report of the Intergovernmental Panel on Climate Change In. [Core Writing Team, R.K. Pachauri and L.A. Meyer (eds.)], Geneva, Switzerland, p. 151.

King, D.A., 2011. Size-Related Changes in Tree Proportions and Their Potential Influence on the Course of Height Growth, in: Size- and Age-Related Changes in Tree Structure and Function, Tree Physiology. Springer, Dordrecht, pp. 165–191. 10.1007/978-94-007-1242-3_6.

Kobe, R.K., 1997. Carbohydrate allocation to storage as a basis of interspecific variation in sapling survivorship and growth. Oikos 80, 226–233. https://doi.org/10.2307/3546590.

Kröber, W., Heklau, H., Bruelheide, H., 2015. Leaf morphology of 40 evergreen and deciduous broadleaved subtropical tree species and relationships to functional ecophysiological traits. Plant Biol. 17, 373–383. https://doi.org/10.1111/plb.12250.

Kurz, W.A., Dymond, C.C., Stinson, G., Rampley, G.J., Neilson, E.T., Carroll, A.L., Ebata, T., Safranyik, L., 2008. Mountain pine beetle and forest carbon feedback to climate change. Nature 452, 987–990. https://doi.org/10.1038/nature06777.

Lai, J., Yang, B., Lin, D., Kerkhoff, A.J., Ma, K., 2013. The allometry of coarse root biomass: log-transformed linear regression or nonlinear regression? PLOS ONE 8, e77007. https://doi.org/10.1371/journal.pone.0077007.

Lloret, F., Sapes, G., Rosas, T., Galiano, L., Saura-Mas, S., Sala, A., Martínez-Vilalta, J., 2018. Non-structural carbohydrate dynamics associated with drought-induced die-off in woody species of a shrubland community. Ann. Bot. 121, 1383–1396. https://doi.org/10.1093/aob/mcy039.

Maguire, A.J., Kobe, R.K., 2015. Drought and shade deplete nonstructural carbohydrate reserves in seedlings of five temperate tree species. Ecol. Evol. 5, 5711–5721. https://doi.org/10.1002/ece3.1819.

Markesteijn, L., Poorter, L., 2009. Seedling root morphology and biomass allocation of 62 tropical tree species in relation to drought- and shade-tolerance. J. Ecol. 97, 311–325. https://doi.org/10.1111/j.1365-2745.2008.01466.x.

Martínez-Vilalta, J., Sala, A., Asensio, D., Galiano, L., Hoch, G., Palacio, S., Piper, F.I., Lloret, F., 2016. Dynamics of non-structural carbohydrates in terrestrial plants: a global synthesis. Ecol. Monogr. 86, 495–516.

McDowell, N., Allen, C.D., Anderson-Teixeira, K., Brando, P., Brienen, R., Chambers, J., Christoffersen, B., Davies, S., Doughty, C., Duque, A., Espirito-Santo, F., Fisher, R., Fontes, C.G., Galbraith, D., Goodsman, D., Grossiord, C., Hartmann, H., Holm, J., Johnson, D.J., Kassim, A.R., Keller, M., Koven, C., Kueppers, L., Kumagai, T., Malhi, Y., McMahon, S.M., Mencuccini, M., Meir, P., Moorcroft, P., Muller-Landau, H.C., Phillips, O.L., Powell, T., Sierra, C.A., Sperry, J., Warren, J., Xu, C., Xu, X., 2018. Drivers and mechanisms of tree mortality in moist tropical forests. New Phytol. 219, 851–869. https://doi.org/10.1111/nph.15027.

McDowell, N.G., Beerling, D.J., Breshears, D.D., Fisher, R.A., Raffa, K.F., Stitt, M., 2011a. The interdependence of mechanisms underlying climate-driven vegetation mortality. Trends Ecol. Evol. 26, 523–532. https://doi.org/10.1016/j.tree.2011.06.003.

McDowell, N.G., Bond, B.J., Dickman, L.T., Ryan, M.G., Whitehead, D., 2011b. Relationships between tree height and carbon isotope discrimination. In: Meinzer, F.C., Lachenbruch, B., Dawson, T.E. (Eds.), Size- and Age-Related Changes in Tree Structure and Function. Tree Physiology. Springer, Dordrecht, pp. 255–286. https://doi.org/10.1007/978-94-007-1242-3_10.

McDowell, N.G., Fisher, R.A., Xu, C., Domec, J.C., Holtta, T., Mackay, D.S., Sperry, J.S., Boutz, A., Dickman, L., Gehres, N., Limousin, J.M., Macalady, A., Martinez-Vilalta, J., Mencuccini, M., Plaut, J.A., Ogee, J., Pangle, R.E., Rasse, D.P., Ryan, M.G., Sevanto, S., Waring, R.H., Williams, A.P., Yepez, E.A., Pockman, W.T., 2013. Evaluating theories of drought-induced vegetation mortality using a multimodel-experiment framework. New Phytol. 200, 304–321. https://doi.org/10.1111/nph.12465.

McDowell, N.G., Grossiord, C., Adams, H.D., Pinzón-Navarro, S., Mackay, D.S., Breshears, D.D., Allen, C.D., Borrego, I., Dickman, L.T., Collins, A., Gaylord, M., McBranch, N., Pockman, W.T., Vilagrosa, A., Aukema, B., Goodsman, D., Xu, C., 2019. Mechanisms of a coniferous woodland persistence under drought and heat. Environ. Res. Lett. 14, 045014. https://doi.org/10.1088/1748-9326/ab0921.

McDowell, N.G., Sevanto, S., 2010. The mechanisms of carbon starvation: how, when, or does it even occur at all? New Phytol. 186, 264–266. https://doi.org/10.1111/j.1469-8137.2010.03232.x.

Mencuccini, M., Martínez-Vilalta, J., Vanderklein, D., Hamid, H.A., Korakaki, E., Lee, S., Michiels, B., 2005. Size-mediated ageing reduces vigour in trees. Ecol. Lett. 8, 1183–1190. https://doi.org/10.1111/j.1461-0248.2005.00819.x.

Mitchell, P.J., O'Grady, A.P., Tissue, D.T., White, D.A., Ottenschlaeger, M.L., Pinkard, E.A., 2013. Drought response strategies define the relative contributions of hydraulic dysfunction and carbohydrate depletion during tree mortality. New Phytol. 197, 862–872. https://doi.org/10.1111/nph.12064.

Mitchell, P.J., O'Grady, A.P., Tissue, D.T., Worledge, D., Pinkard, E.A., 2014. Co-ordination of growth, gas exchange and hydraulics define the carbon safety margin in tree species with contrasting drought strategies. Tree Physiol. 34, 443–458. https://doi.org/10.1093/treephys/tpu014.

Mueller, R.C., Scudder, C.M., Porter, M.E., Talbot Trotter, R., Gehring, C.A., Whitham, T.G., 2005. Differential tree mortality in response to severe drought: evidence for

long-term vegetation shifts. J. Ecol. 93, 1085–1093. https://doi.org/10.1111/j.1365-2745.2005.01042.x.
Nardini, A., Casolo, V., Dal Borgo, A., Savi, T., Stenni, B., Bertoncin, P., Zini, L., McDowell, N.G., 2016. Rooting depth, water relations and non-structural carbohydrate dynamics in three woody angiosperms differentially affected by an extreme summer drought: Rooting depth and plant hydraulics. Plant Cell Environ. 39, 618–627. https://doi.org/10.1111/pce.12646.
Niinemets, Ü., 2010. Responses of forest trees to single and multiple environmental stresses from seedlings to mature plants: Past stress history, stress interactions, tolerance and acclimation. For. Ecol. Manag. 260, 1623–1639. https://doi.org/10.1016/j.foreco.2010.07.054.
Oberhuber, W., Hammerle, A., Kofler, W., 2015. Tree water status and growth of saplings and mature Norway spruce (Picea abies) at a dry distribution limit. Front. Plant Sci. 6. https://doi.org/10.3389/fpls.2015.00703.
O'Brien, M.J., Burslem, D.F.R.P., Caduff, A., Tay, J., Hector, A., 2015. Contrasting non-structural carbohydrate dynamics of tropical tree seedlings under water deficit and variability. New Phytol. 205, 1083–1094. https://doi.org/10.1111/nph.13134.
O'Brien, M.J., Leuzinger, S., Philipson, C.D., Tay, J., Hector, A., 2014. Drought survival of tropical tree seedlings enhanced by non-structural carbohydrate levels. Nat. Clim. Change 4, 710–714. https://doi.org/10.1038/nclimate2281.
Olson, M.E., Soriano, D., Rosell, J.A., Anfodillo, T., Donoghue, M.J., Edwards, E.J., León-Gómez, C., Dawson, T., Martínez, J.J.C., Castorena, M., Echeverría, A., Espinosa, C.I., Fajardo, A., Gazol, A., Isnard, S., Lima, R.S., Marcati, C.R., Méndez-Alonzo, R., 2018. Plant height and hydraulic vulnerability to drought and cold. Proc. Natl. Acad. Sci. 115, 7551–7556. https://doi.org/10.1073/pnas.1721728115.
Palacio, S., Millard, P., Maestro, M., Montserrat-Marti, G., 2007. Non-structural carbohydrates and nitrogen dynamics in Mediterranean sub-shrubs: an analysis of the functional role of overwintering leaves. Plant Biol. 9, 49–58. https://doi.org/10.1055/s-2006-924224.
Phillips, O.L., Aragão, L.E.O.C., Lewis, S.L., Fisher, J.B., Lloyd, J., López-González, G., Malhi, Y., Monteagudo, A., Peacock, J., Quesada, C.A., van der Heijden, G., Almeida, S., Amaral, I., Arroyo, L., Aymard, G., Baker, T.R., Bánki, O., Blanc, L., Bonal, D., Brando, P., Chave, J., de Oliveira, A.C.A., Cardozo, N.D., Czimczik, C.I., Feldpausch, T.R., Freitas, M.A., Gloor, E., Higuchi, N., Jiménez, E., Lloyd, G., Meir, P., Mendoza, C., Morel, A., Neill, D.A., Nepstad, D., Patiño, S., Peñuela, M.C., Prieto, A., Ramírez, F., Schwarz, M., Silva, J., Silveira, M., Thomas, A.S., Steege, H.T., Stropp, J., Vásquez, R., Zelazowski, P., Alvarez Dávila, E., Andelman, S., Andrade, A., Chao, K.-J., Erwin, T., Di Fiore, A., Honorio C, E., Keeling, H., Killeen, T.J., Laurance, W.F., Peña Cruz, A., Pitman, N.C.A., Núñez Vargas, P., Ramírez-Angulo, H., Rudas, A., Salamão, R., Silva, N., Terborgh, J., Torres-Lezama, A., 2009. Drought sensitivity of the Amazon rainforest. Science 323, 1344–1347. 10.1126/science.1164033.
Piper, F.I., 2011. Drought induces opposite changes in the concentration of non-structural carbohydrates of two evergreen Nothofagus species of differential drought resistance. Ann. For. Sci. 68, 415–424. https://doi.org/10.1007/s13595-011-0030-1.
Piper, F.I., Fajardo, A., 2016. Carbon dynamics of Acer pseudoplatanus seedlings under drought and complete darkness. Tree Physiol. 36, 1400–1408. https://doi.org/10.1093/treephys/tpw063.
Piper, F.I., Fajardo, A., Hoch, G., 2017. Single-provenance mature conifers show higher non-structural carbohydrate storage and reduced growth in a drier location. Tree Physiol. 37, 1001–1010. https://doi.org/10.1093/treephys/tpx061.
R Development Core Team, 2018. R: A Language and Environment for Statistical Computing. R Foundation for Statistical Computing, Vienna, Austria.
Rodríguez-Calcerrada, J., Li, M., López, R., Cano, F.J., Oleksyn, J., Atkin, O.K., Pita, P., Aranda, I., Gil, L., 2017. Drought-induced shoot dieback starts with massive root xylem embolism and variable depletion of nonstructural carbohydrates in seedlings of two tree species. New Phytol. 213, 597–610. https://doi.org/10.1111/nph.14150.
Rosas, T., Galiano, L., Ogaya, R., Penuelas, J., Martinez-Vilalta, J., 2013. Dynamics of non-structural carbohydrates in three Mediterranean woody species following long-term experimental drought. Front. Plant Sci. 4, 400. https://doi.org/10.3389/fpls.2013.00400.
Rowland, L., da Costa, A.C.L., Galbraith, D.R., Oliveira, R.S., Binks, O.J., Oliveira, A.A.R., Pullen, A.M., Doughty, C.E., Metcalfe, D.B., Vasconcelos, S.S., Ferreira, L.V., Malhi, Y., Grace, J., Mencuccini, M., Meir, P., 2015. Death from drought in tropical forests is triggered by hydraulics not carbon starvation. Nature 528, 119–122. 10.1038/nature15539.
Sala, A., Piper, F., Hoch, G., 2010. Physiological mechanisms of drought-induced tree mortality are far from being resolved. New Phytol. 186, 274–281. https://doi.org/10.1111/j.1469-8137.2009.03167.x.
Smith, M.N., Stark, S.C., Taylor, T.C., Ferreira, M.L., de Oliveira, E., Restrepo-Coupe, N., Chen, S., Woodcock, T., dos Santos, D.B., Alves, L.F., Figueira, M., de Camargo, P.B., de Oliveira, R.C., Aragão, L.E.O.C., Falk, D.A., McMahon, S.M., Huxman, T.E., Saleska, S.R., 2019. Seasonal and drought-related changes in leaf area profiles depend on height and light environment in an Amazon forest. New Phytol. 222, 1284–1297. https://doi.org/10.1111/nph.15726.
Stovall, A.E.L., Shugart, H., Yang, X., 2019. Tree height explains mortality risk during an intense drought. Nature Commun. 10, 1–6. https://doi.org/10.1038/s41467-019-12380-6.
Tang, X., Fehrmann, L., Guan, F., Forrester, D.I., Guisasola, R., Pérez-Cruzado, C., Vor, T., Lu, Y., Álvarez-González, J.G., Kleinn, C., 2017. A generalized algebraic difference approach allows an improved estimation of aboveground biomass dynamics of Cunninghamia lanceolata and Castanopsis sclerophylla forests. Ann. For. Sci. 74, 12. https://doi.org/10.1007/s13595-016-0603-0.
Thomas, S.C., Winner, W.E., 2002. Photosynthetic differences between saplings and adult trees: an integration of field results by meta-analysis. Tree Physiol. 22, 117–127. https://doi.org/10.1093/treephys/22.2-3.117.
Trugman, A.T., Detto, M., Bartlett, M.K., Medvigy, D., Anderegg, W.R.L., Schwalm, C., Schaffer, B., Pacala, S.W., 2018. Tree carbon allocation explains forest drought-kill and recovery patterns. Ecol. Lett. 21, 1552–1560. https://doi.org/10.1111/ele.13136.
Wiley, E., King, C.M., Landhäusser, S.M., 2019. Identifying the relevant carbohydrate storage pools available for remobilization in aspen roots. Tree Physiol. 39, 1109–1120. https://doi.org/10.1093/treephys/tpz051.
Xu, M., 2008. The study of forest canopy structure and photosynthesis in subtropical evergreen broad-leaved forest communities. Mater thesis. Easter China Normal University, Shanghai (in Chinese with English abstract).
Yan, E.-R., Wang, X.-H., Huang, J.-J., 2006. Shifts in plant nutrient use strategies under secondary forest succession. Plant Soil 289, 187–197. https://doi.org/10.1007/s11104-006-9128-x.
Yang, B., Wen, X., Sun, X., 2015. Seasonal variations in depth of water uptake for a subtropical coniferous plantation subjected to drought in an East Asian monsoon region. Agric. For. Meteorol. 201, 218–228. https://doi.org/10.1016/j.agrformet.2014.11.020.
Yang, T., Song, K., Da, L., Li, X., Wu, J., 2010. The biomass and aboveground net primary productivity of Schima superba-Castanopsis carlesii forests in east China. Sci. China Life Sci. 53, 811–821. https://doi.org/10.1007/s11427-010-4021-5.
Zeng F., Shi J., Yan E., Zhang R., Wang X., Fan-rong Z., Jia-yue S.H.I., En-rong Y.A.N., Ren-liang Z., Xi-hua W., 2008. Temporal and spatial patterns of fine root mass along a secondary succession of evergreen broad-leaved forest in Tiantong (Chinese). J. East China Norm. Univ. Sci. 2008, 56.
Zhang, H., Wang, C., Wang, X., 2014. Spatial variations in non-structural carbohydrates in stems of twelve temperate tree species. Trees 28, 77–89. https://doi.org/10.1007/s00468-013-0931-8.
Zhang, J., Wen, G., Zhang, M., Liu, X., 2012. Autumnal water features of eight tree species in Zhejiang. J. Zhejiang Af Univ. 29, 35–40. 10.11833/j.issn.2095-0756.2012.01.007.
Zhang, Y.-J., Meinzer, F.C., Hao, G.-Y., Scholz, F.G., Bucci, S.J., Takahashi, F.S.C., Villalobos-Vega, R., Giraldo, J.P., Cao, K.-F., Hoffmann, W.A., Goldstein, G., 2009. Size-dependent mortality in a Neotropical savanna tree: the role of height-related adjustments in hydraulic architecture and carbon allocation. Plant Cell Environ. 32, 1456–1466. https://doi.org/10.1111/j.1365-3040.2009.02012.x.
Zhou, G., Zhou, X., Zhang, T., Du, Z., He, Y., Wang, X., Shao, J., Cao, Y., Xue, S., Wang, H., Xu, C., 2017. Biochar increased soil respiration in temperate forests but had no effects in subtropical forests. For. Ecol. Manag. 405, 339–349. https://doi.org/10.1016/j.foreco.2017.09.038.
Zuo, S., Ren, Y., Weng, X., Ding, H., Luo, Y., 2015. Biomass allometric equations of nine common tree species in an evergreen broadleaved forest of subtropical China. Yingyong Shengtai Xuebao 26.
Zweifel, R., Item, H., Häsler, R., 2000. Stem radius changes and their relation to stored water in stems of young Norway spruce trees. Trees 15, 50–57. https://doi.org/10.1007/s004680000072.